Diagnostic Accuracy Study

Medicine®

OPEN

Reduction of the radiation dose and the amount of contrast material in hepatic dynamic CT using low tube voltage and adaptive iterative dose reduction 3-dimensional

Atsushi Nakamoto, MD, PhD[a,b,*], Kiyohito Yamamoto, MD, PhD[a], Makoto Sakane, MD, PhD[a], Go Nakai, MD, PhD[a], Akira Higashiyama, MD[a], Hiroshi Juri, MD, PhD[a], Shushi Yoshikawa, RT[c], Yoshifumi Narumi, MD, PhD[a]

Abstract

The purpose of this study was to prospectively evaluate the image quality and the diagnostic ability of low tube voltage and reduced contrast material dose hepatic dynamic computed tomography (CT) reconstructed with adaptive iterative dose reduction 3-dimensional (AIDR 3D).

Eighty-nine patients underwent hepatic dynamic CT using one of the 2 protocols: tube voltage of 120 kVp, contrast dose of 600 mgI/kg, and filtered back projection in Protocol A (n = 46), and tube voltage of 100 kVp, contrast dose of 500 mgI/kg, and AIDR 3D in Protocol B (n = 43). The volume CT dose index ($CTDI_{vol}$) and size-specific dose estimates (SSDEs) were compared between the 2 groups. Objective image noise and tumor to liver contrast-to-noise ratio (CNR) were also compared. Three radiologists independently reviewed image quality. The jackknife alternative free-response receiver-operating characteristic (JAFROC) analysis was performed to compare diagnostic performance.

The mean $CTDI_{vol}$ and SSDE of Protocol B (14.3 and 20.2, respectively) were significantly lower than those of Protocol A (22.1 and 31.4, $P < .001$). There were no significant differences in either objective image noise or CNR. In the qualitative analysis, 2 readers assigned significant lower scores to images of Protocol B for at least one of the 3 phases regarding overall image quality ($P < .05$). There was no significant difference in the JAFROC1 figure of merit between protocols.

Low tube voltage CT with AIDR 3D yielded a reduction in radiation dose and in the amount of contrast material while maintaining diagnostic performance.

Abbreviations: AIDR 3D = adaptive iterative dose reduction 3-dimensional, AP = arterial phase, CT = computed tomography, $CTDI_{vol}$ = volume CT dose index, DLP = dose length product, EP = equilibrium phase, FBP = filtered back projection, FOM = figure of merit, HCC = hepatocellular carcinoma, IR = iterative reconstruction, PPV = positive predictive value, PVP = portal venous phase, ROI = regions of interest, TACE = transcatheter arterial chemoembolization.

Keywords: computed tomography, dose reduction, iterative reconstruction, liver, low tube voltage

1. Introduction

Reducing radiation dose in computed tomography (CT) is essential as an increase in the number of examinations over the past few decades has resulted in an increased risk of radiation-induced carcinogenesis.[1,2] The use of low tube voltage CT is a promising technique which increases the X-ray absorption of iodine and thus improves iodine enhancement of vascular and parenchymal structures, while simultaneously reducing patient radiation exposure.[3,4] Previous studies have shown the utility of low tube voltage CT for hypervascular hepatocellular carcinoma (HCC) detection,[3,5–8] but the increased image noise associated with the technique is problematic.

Recently, iterative reconstruction (IR) has been used as an alternative algorithm for the reconstruction of CT images. IR can reduce image noise compared to filtered back projection (FBP), the standard reconstruction algorithm. Some reports have shown that low tube voltage hepatic dynamic CT with hybrid IR, which involves blending with FBP to keep the noise characteristics and image textures, could reduce both radiation dose and the amount of iodine contrast material.[9–16]

Adaptive iterative dose reduction 3-dimensional (AIDR 3D; Toshiba Medical Systems, Otawara, Japan) is a hybrid IR algorithm, which has already been used in abdominal and pelvic CT with reduced dose scans.[17–25] However, the combination of hepatic dynamic CT with low tube voltage technique and AIDR 3D has not been investigated. Moreover, to our knowledge, there are no previous reports which have evaluated the diagnostic

Editor: Hyunjin Park.

This work was supported by a grant from Toshiba Medical Systems and Eisai.

The authors have no conflicts of interest to disclose.

[a] Department of Radiology, Osaka Medical College, Takatsuki, [b] Department of Radiology, Osaka University Graduate School of Medicine, Suita, [c] Central Radiology Department, Osaka Medical College Hospital, Takatsuki, Osaka, Japan.

[*] Correspondence: Atsushi Nakamoto, Department of Radiology, Osaka University Graduate School of Medicine, Suita, Osaka 565-0871, Japan (e-mail: a-nakamoto@radiol.med.osaka-u.ac.jp)

Copyright © 2018 the Author(s). Published by Wolters Kluwer Health, Inc. This is an open access article distributed under the terms of the Creative Commons Attribution-Non Commercial-No Derivatives License 4.0 (CCBY-NC-ND), where it is permissible to download and share the work provided it is properly cited. The work cannot be changed in any way or used commercially without permission from the journal.

Medicine (2018) 97:34(e11857)

Received: 4 March 2018 / Accepted: 20 July 2018

http://dx.doi.org/10.1097/MD.0000000000011857

ability of low tube voltage hepatic dynamic CT with IR using a free-response methodology such as the jackknife free-response receiver-operating characteristic (JAFROC) analysis, which has been reported to yield greater statistical power at detecting modality differences.[26–28]

The purpose of this study was to prospectively evaluate the image quality and diagnostic performance of low tube voltage and reduced contrast material dose hepatic dynamic CT reconstructed with AIDR 3D, and compare it with standard tube voltage and standard contrast material dose CT with FBP.

2. Materials and methods

2.1. Patients

This prospective study was approved by our institutional review board, and written informed consent was obtained from all patients. Between May 2015 and May 2016, 90 consecutive patients who were scheduled to undergo hepatic dynamic CT with a 320-slice CT scanner for the evaluation of known or suspected HCC were enrolled in the study. One patient was excluded from the following analyses because almost the entire liver was occupied by multiple tumors and was deemed to be difficult to analyze. The remaining 89 patients (49 men and 40 women, age range, 40–80 years; mean age, 70.6 years) were included in the study. The body mass index (BMI) of the patients ranged from 15.8 to 35.7 (mean, 22.9). The clinical indications for hepatic dynamic CT were as follows: hepatitis B (n = 4), hepatitis C (n = 17), follow-up after surgery for HCC (n = 32), follow-up after radiofrequency ablation for HCC (n = 22), follow-up after transcatheter arterial chemoembolization (TACE) for HCC (n = 4), alcoholic hepatitis (n = 3), nonalcoholic steatohepatitis (n = 4), primary biliary cirrhosis (n = 2), and autoimmune hepatitis (n = 1).

2.2. Lesion reference standards

Five HCCs in 4 patients were pathologically diagnosed after the surgery. For the other patients, the diagnosis of HCC was made by 2 radiologists experienced in abdominal radiology (7 and 13 years, respectively) by consensus when a lesion was enhanced on arterial phase CT images and met one of the following criteria: an increase in size in follow-up CT, contrast enhanced on the arterial phase and low intensity on the hepatobiliary phase images of gadoxetic acid-enhanced magnetic resonance imaging (MRI), concentration of lipiodol after TACE, and a decrease in size after TACE with drug-eluting beads. The absence of HCC was confirmed when no HCC was detected on follow-up CT or MRI (more than 6 months after the initial CT), or on follow-up ultrasound (more than 12 months after the initial CT). A total of 77 HCCs in 24 patients were diagnosed, whereas no HCC was detected in 44 patients. The remaining 21 patients did not have any follow-up examinations which fulfill the criteria mentioned above and were excluded from the analysis of the diagnostic performance. The diameter of HCCs ranged from 4 to 64 mm (mean, 13.5 mm, standard deviation [SD], 10.5).

2.3. CT examination

Hepatic dynamic CT was performed using a 320-slice scanner (AquilionONE; Toshiba Medical Systems). All patients were randomly assigned to one of the 2 protocols with different tube voltages and amounts of contrast material (Table 1). Of the 89 patients, 46 were scanned with Protocol A, while the other 43 were scanned with Protocol B. Mean patients' BMI was not significantly different between the 2 protocols (22.8 and 23.1 for Protocols A and B, respectively, $P = .74$ [Student t test]). All patients underwent a precontrast scan and a contrast-enhanced dynamic scan including the arterial phase (AP), portal venous phase (PVP), and equilibrium phase (EP). Nonionic contrast material (Iomeron; Eisai, Tokyo, Japan) was administered intravenously for 30 seconds by means of a power injector (Dual Shot GX; Nemoto Kyorindo, Tokyo, Japan). The scanning delays of the AP were individually determined by using a bolus-tracking technique. A circular cursor was placed on the aorta, and the AP scan was started 20 seconds after a threshold of 200 Hounsfield Unit (HU) was reached. The PVP was acquired 30 seconds after the AP scan, and the EP was acquired 180 seconds after the start of administration of the contrast material.

Axial images of 5 mm thickness were reconstructed with 5 mm intervals using FBP and AIDR 3D (AIDR 3D Weak, available only in Japan) for Protocols A and B, respectively.

Table 1

Acquisition and reconstruction parameters of computed tomography examination.

	Protocol A	Protocol B
Acquisition protocol		
Tube voltage, kVp	120	100
Tube current	Auto exposure control	
SD of the image noise	10	11
Beam collimation, mm	64×0.5	
Helical pitch	0.828	
Rotation time, s	0.5	
Scan field of view, mm	320 or 400	
Amount of contrast material, mgI/kg	600	500
Reconstruction protocol		
Reconstruction algorithm	FBP	AIDR 3D
Reconstruction field of view, mm	320 or 360 or 400	
Kernel	FC13	
Slice thickness/interval, mm	5/5	

AIDR 3D = adaptive iterative dose reduction 3-dimensional, FBP = filtered back projection, SD = standard deviation.

2.4. Radiation dose assessment

The volume CT dose index ($CTDI_{vol}$, mGy) and the dose length product (DLP, mGy cm) were recorded as per the dose reports. Anteroposterior thickness at the midline and lateral width were measured from axial images for each patient, and size-specific dose estimates (SSDEs) were calculated using $CTDI_{vol}$ and tabulated size-dependent conversion factors (f_{size}).[29,30]

2.5. Quantitative analysis

The radiologist placed circular regions of interest (ROI) of approximately 100 mm^2 on the liver parenchyma, and the average and SD of the CT number were recorded for each phase. Three ROIs were placed per phase, and their values averaged. If any HCCs were present, the CT numbers of HCCs were also recorded. The SD of the CT number of liver parenchyma was used as the index of image noise. The lesion to liver contrast-to-noise ratio (CNR) was calculated using the following equation:

$$CNR = (CT_{HCC} - CT_{Liver})/SD_{Liver}$$

where CT_{HCC} and CT_{Liver} are the CT numbers of the HCC and liver parenchyma, respectively. SD_{Liver} is the SD of the CT numbers of the liver parenchyma.

2.6. Qualitative analysis

Three radiologists, other than the 2 radiologists who evaluated the reference standards of HCCs, independently reviewed the contrast-enhanced images of each phase, and evaluated the image quality in terms of the degree of noise, sharpness, and overall image quality. They had 6, 11, and 11 years experience in abdominal radiology. They were informed that patients were suspected of having HCCs and scanned with the 120 kVp or 100 kVp setting, but they were blinded to the numbers and the places of lesions, scanning protocol and reconstruction algorithm. A commercially available workstation (Ziostation 2 version 2.4.0.3; Ziosoft, Tokyo, Japan) was used for the assessment. The degree of noise was graded using a 4-point scale in which a score of 1 indicated unacceptable image noise and 4 indicated minimum noise. Sharpness was assessed by the sharpness of abdominal visceral structures using a 4-point scale in which a score of 1 represented the most blurred and 4 represented the sharpest image. Overall image quality was also rated using a 4-point scale: 1 = poor, 2 = fair, 3 = good, and 4 = excellent. For all assessments, a score of 3 indicated an equivalent image quality to that of CT images used in routine practice.

To evaluate the diagnostic performance, they reviewed the precontrast images and the contrast-enhanced images of each phase together, and evaluated the possible presence of hypervascular HCC. They classified all detected lesions which were likely hypervascular HCC using the following 4-point confidence score scale: 1 = probably no lesion present, 2 = indefinite presence of lesion, 3 = lesion probably present, and 4 = lesion definitely present. Hypovascular HCC was not evaluated in this study. Before the assessment, they were informed that only a confidence level of 3 or 4 would be considered a positive finding for the calculation of sensitivity and positive predictive value (PPV).

2.7. Statistical analysis

Mean $CTDI_{vol}$, DLP, and SSDE between the 2 protocols were statistically compared using the Student *t* test. The CT number of liver parenchyma, objective image noise, and CNR of HCC were also compared using the Student *t* test. Mean visual score was compared between the 2 protocols using the Mann–Whitney *U* test. The Spearman correlation coefficient by rank test was used for the evaluation of the correlation between the visual scores of overall image quality and BMI for each protocol.

To analyze the diagnostic performance of hypervascular HCC, JAFROC was performed using the JAFROC software (JAFROC version 4.2.1, www.devchakraborty.com). This software computes a figure of merit (FOM), which is defined as the probability that a lesion is rated higher than the highest rated nonlesion on a normal image. The JAFROC1 method was used in this study, instead of JAFROC or JAFROC2, due to its high statistical power for human observers.[28,31] Mean FOM, sensitivity (for all lesions, lesions ≥1.0 cm, and lesions <1.0 cm), and PPV were compared using the Student *t* test between the 2 protocols.

For all tests, a *P*-value <.05 was considered significant.

3. Results

3.1. Radiation dose assessment

Mean $CTDI_{vol}$, DLP, and SSDE are summarized in Table 2. Mean $CTDI_{vol}$, DLP, and SSDE for Protocol B were significantly lower than those for Protocol A ($P < .001$). Mean SSDE of Protocol B was 36% less than that of Protocol A.

Table 2

Mean $CTDI_{vol}$, DLP, and SSDE of each protocol.

	Protocol A (120 kVp, FBP)	Protocol B (100 kVp, AIDR 3D)	*P*
$CTDI_{vol}$, mGy	22.1 ± 6.4	14.3 ± 3.5	<.001
DLP, mGy·cm	607.2 ± 214.2	376.5 ± 109.3	<.001
SSDE, mGy	31.4 ± 6.4	20.2 ± 3.4	<.001

Data are presented as mean ± standard deviation.

AIDR 3D = adaptive iterative dose reduction 3-dimensional, FBP = filtered back projection, $CTDI_{vol}$ = volume computed tomography dose index, DLP = dose length product, SSDE = size-specific dose estimate.

3.2. Quantitative analysis

There was no significant difference in mean CT number of liver parenchyma between the 2 protocols, although Protocol B tended to have higher CT numbers (Table 3). The image noise of Protocol B in the AP was significantly lower than that of Protocol A ($P < .05$), whereas there was no significant difference between the 2 protocols in PVP and EP. There was no significant difference in CNR between the 2 protocols except for the EP ($P < .05$).

3.3. Qualitative analysis

Mean scores for image noise, image sharpness, and overall image quality in the qualitative analysis are summarized in Table 4. Regarding scores for image noise, there was no significant difference between the 2 protocols in any phase for Reader 1, whereas Readers 2 and 3 assigned significantly lower scores to Protocol B in all phases ($P < .05$). For image sharpness, a significant difference between the 2 protocols was found only in the AP for Reader 2 ($P < .05$). For overall image quality, Readers 2 and 3 assigned significant lower scores to Protocol B in at least 1 of 3 phases, including the AP ($P < .05$) (Fig. 1). For Protocol A, a significant positive correlation was found between scores of overall image quality and BMI in PVP and EP for Reader 3 ($P < .05$), whereas no significant correlation was found for the other readers. For Protocol B, no significant correlation was found between visual scores and BMI for all readers.

Table 3

Mean CT number of the liver, image noise, and CNR for each protocol.

	Protocol A (120 kVp, FBP)	Protocol B (100 kVp, AIDR 3D)	*P*
CT number of the liver (HU)			
AP	81.6 ± 13.0	85.0 ± 13.8	.88
PVP	116.8 ± 10.8	118.6 ± 16.7	.73
EP	98.7 ± 7.6	101.4 ± 11.9	.90
Image noise (HU)			
AP	10.6 ± 1.8	10.0 ± 0.7	.02
PVP	10.7 ± 1.7	10.3 ± 1.0	.05
EP	10.5 ± 1.7	10.2 ± 0.9	.12
CNR			
AP	3.0 ± 1.5	3.6 ± 1.9	.11
PVP	0.1 ± 1.1	−0.4 ± 1.2	.06
EP	−0.5 ± 1.1	−0.9 ± 0.9	.04

Data are mean ± standard deviation.

AIDR 3D = adaptive iterative dose reduction 3-dimensional, AP = arterial phase, CNR = contrast-to-noise ratio, CT = computed tomography, EP = equilibrium phase, FBP = filtered back projection, PVP = portal venous phase.

Table 4

Mean visual scores of image noise, image sharpness, and over all image quality.

	Reader 1			Reader 2			Reader 3		
	Protocol A	Protocol B	*P*	Protocol A	Protocol B	*P*	Protocol A	Protocol B	*P*
Image noise									
AP	2.8±0.4	2.9±0.3	.13	3.0±0.2	2.7±0.4	<.01	2.9±0.3	2.7±0.5	.04
PVP	2.8±0.4	2.9±0.3	.08	3.0±0.1	2.7±0.5	<.001	2.9±0.3	2.7±0.4	.01
EP	2.6±0.5	2.8±0.4	.07	3.0±0.2	2.7±0.5	<.01	2.8±0.4	2.4±0.5	<.001
Sharpness									
AP	3.0±0	3.0±0	.99	3.0±0	2.9±0.3	.02	3.0±0.2	2.9±0.3	.15
PVP	3.0±0	3.0±0	.99	3.0±0	3.0±0.2	.30	2.9±0.3	2.9±0.3	.93
EP	3.0±0	3.0±0	.99	3.0±0	3.0±0.2	.30	3.0±0.2	3.0±0.2	.96
Overall image quality									
AP	3.0±0	3.0±0.2	.30	3.0±0	2.9±0.3	.04	3.0±0.2	2.9±0.4	.04
PVP	3.0±0	3.0±0	.99	3.0±0	3.0±0.2	.14	3.0±0.2	2.9±0.3	.35
EP	3.0±0	3.0±0.2	.30	3.0±0	3.0±0.2	.14	3.0±0.2	2.8±0.4	.02

AP = arterial phase, EP = equilibrium phase, PVP = portal venous phase.

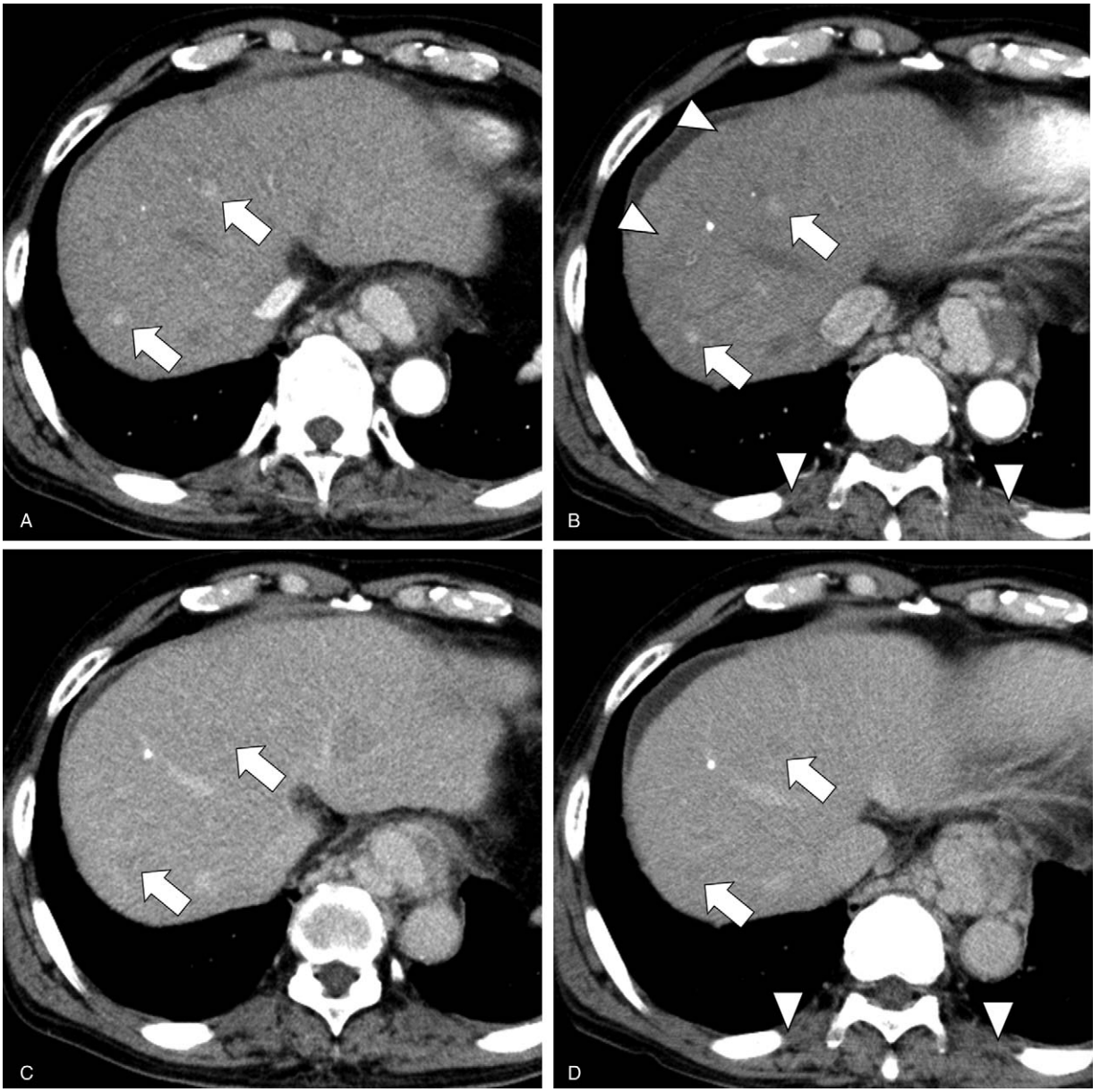

Figure 1. A male in his sixties who underwent hepatic dynamic computed tomography with both Protocols A and B within 3 months. The conspicuity of 2 hepatocellular carcinomas (arrows) in arterial phase images (A: Protocol A; B: Protocol B) and equilibrium phase images (C: Protocol A; D: Protocol B) is almost equivalent for these 2 protocols. Streak artifacts caused by ribs and spine are slightly more prominent in Protocol B (arrowhead).

Table 5

Figure of merit, sensitivity, and positive predictive value for the detection of hypervascular hepatocellular carcinoma.

	Protocol A (120 kVp, FBP)	Protocol B (100 kVp, AIDR 3D)	*P*
Figure of merit			
Reader 1	0.60	0.65	
Reader 2	0.66	0.70	
Reader 3	0.69	0.65	
Mean	0.65	0.67	.69
Sensitivity (all lesions)			
Reader 1	0.21 (6/28)	0.29 (14/49)	
Reader 2	0.32 (9/28)	0.35 (17/49)	
Reader 3	0.36 (10/28)	0.39 (19/49)	
Mean	0.30	0.34	.95
Sensitivity (lesions $\geq$ 1.0 cm)			
Reader 1	0.46 (6/13)	0.46 (13/28)	
Reader 2	0.46 (6/13)	0.50 (14/28)	
Reader 3	0.69 (9/13)	0.64 (18/28)	
Mean	0.54	0.54	.46
Sensitivity (lesions $<$ 1.0 cm)			
Reader 1	0.00 (0/15)	0.05 (1/21)	
Reader 2	0.20 (3/15)	0.14 (3/21)	
Reader 3	0.07 (1/15)	0.05 (1/21)	
Mean	0.09	0.08	.39
Positive predictive value			
Reader 1	0.75 (6/8)	1.00 (14/14)	
Reader 2	0.90 (9/10)	0.94 (17/18)	
Reader 3	0.91 (10/11)	0.95 (19/20)	
Mean	0.85	0.96	.88

Numbers in parentheses are actual numbers of lesions.
AIDR 3D = adaptive iterative dose reduction 3-dimensional, FBP = filtered back projection.

The FOM, sensitivity, and PPV for the detection of hypervascular HCC are summarized in Table 5. Mean FOM, sensitivity for all lesions, and PPV of Protocol B were higher than those of Protocol A, although the differences were not significant. Mean sensitivities for lesions $\geq$1.0 cm and for $<$1.0 cm were not significantly different between the 2 protocols.

4. Discussion

Our results demonstrate that low tube voltage (100 kVp) CT could yield a significant dose reduction compared to standard tube voltage (120 kVp) CT, and that SSDE could be reduced by 36% using the 100 kVp protocol. Meanwhile, the objective image noise of 100 kVp images was significantly lower in the AP and PVP, and the CNR in the AP was not significantly different between the 2 protocols. Thus, the use of AIDR 3D compensated the increase of the image noise associated with the use of the low tube voltage technique, therefore maintaining the objective image quality. These results were concordant with previous reports which also used the combination of low tube voltage and a hybrid IR of other manufacturers.[11,12,14,15]

However, visual scores of the subjective image noise of Protocol B were significantly lower than those of Protocol A in all of 3 phases for Readers 2 and 3. Regarding the overall image quality, Reader 2 assigned significantly lower scores for Protocol B in the AP, and Reader 3 do so in the AP and EP. A reason for the lower visual scores of the low tube voltage images might be the "pixelated blotchy" appearance, which has been reported as a frequently observed artifact in images reconstructed using IR algorithms[32,33] and can result in an unfamiliar image texture for radiologists. Although a relatively low strength of the IR preset (AIDR 3D Weak, available only in Japan) was used in the present study, a pixelated blotchy appearance was observed in some patients, whose images might be considered lower quality (Fig. 2). However, no patient images of Protocol B were labeled unacceptable (i.e., a score of 1), and the majority of the images were assigned a score of 3, which meant an image quality equal to those of images from routine clinical practice. Although increased image noise of low tube voltage CT would be problematic in heavier patients,[4–6] no negative correlation was found between the visual scores and BMI for the 100 kVp setting in our study.

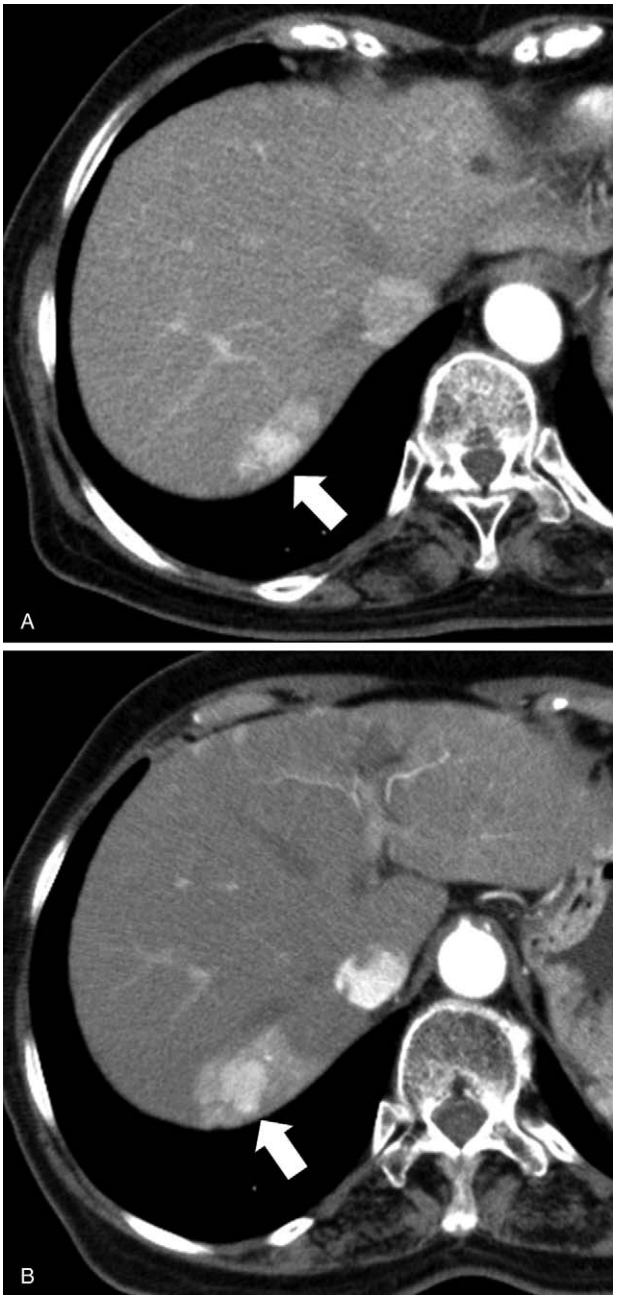

Figure 2. Initial computed tomography (CT) (A: Protocol B) and follow-up CT (B: Protocol A) images of a female in her seventies with hepatocellular carcinoma. The contrast between the hepatocellular carcinoma and the liver parenchyma is almost equivalent for both protocols. A faint blotchy appearance may be seen in Protocol B.

This may be because our study population did not include any extremely heavy patients (maximum BMI, 35.7). However, our results suggested that 100 kVp setting with AIDR 3D would provide acceptable image quality for relatively heavy patients with BMI of around 30.

When a reduced-dose protocol is applied, it would be a more important consideration to maintain diagnostic performance rather than objective or subjective image quality. However, most previous studies investigating the combination of low tube voltage and IR for hepatic dynamic CT were focused on image quality, with few reports investigating diagnostic capability in a blinded fashion.[15] Our results showed no significant differences between the 2 protocols regarding FOM, sensitivity, and PPV for the detection of hypervascular HCC. Thus, the 100 kVp protocol with AIDR 3D for the hepatic dynamic CT, which decreases both the radiation dose and the amount of contrast material, would be acceptable in terms of the diagnostic performance.

Some previous studies have shown that hybrid IRs do not improve the detection of low-contrast lesions on reduced-dose abdominal CT.[34–38] Therefore, the preservation of the diagnostic performance may be simply due to the higher contrast enhancement of hypervascular HCC on lower tube voltage images. We did not compare the image quality and diagnostic capability between FBP and AIDR 3D for the same low tube voltage setting (i.e., 100 kVp), and further studies would be needed to determine the actual effect of a hybrid IR on the diagnostic performance of hypervascular HCC on low tube voltage hepatic dynamic CT.

This study had several limitations. First, the number of patients with HCC was relatively small, and histopathologic confirmation was not proved in many cases. A larger patient population would be needed to confirm the equivalence of the 2 protocols. Second, the mean body weight of the patients in our study was 58.4 kg, which is smaller than North American and European matched populations. Third, we investigated only the combination of the 100 kVp, 500 mgI/kg, SD = 11, and AIDR 3D weak. Many studies have reported low tube voltage hepatic dynamic CT with 80 kVp,[3,5–13,15] which might enable a protocol with an even lower dose of contrast material. As we intended to maintain image quality and texture on the low tube voltage images, we avoided the lower voltage and a stronger IR setting. Moreover, we did not evaluate the effect of AIDR 3D on the 120 kVp images. The optimal combination of tube voltage, amount of contrast material, SD setting, and IR level would need to be investigated on a separate study.

In conclusion, low tube voltage CT with AIDR 3D yielded a reduction in radiation dose and the amount of contrast material while maintaining the objective image noise and diagnostic performance for hypervascular HCC compared to standard tube voltage CT with FBP.

Author contributions

Conceptualization: Atsushi Nakamoto, Shushi Yoshikawa, Yoshifumi Narumi.
Data curation: Atsushi Nakamoto, Kiyohito Yamamoto, Makoto Sakane, Go Nakai, Akira Higashiyama, Hiroshi Juri, Shushi Yoshikawa.
Formal analysis: Atsushi Nakamoto.
Funding acquisition: Yoshifumi Narumi.
Investigation: Atsushi Nakamoto, Kiyohito Yamamoto, Makoto Sakane, Go Nakai, Shushi Yoshikawa.
Methodology: Atsushi Nakamoto, Shushi Yoshikawa.
Project administration: Atsushi Nakamoto.
Supervision: Yoshifumi Narumi.
Writing – original draft: Atsushi Nakamoto.
Writing – review & editing: Yoshifumi Narumi.

References

[1] Brenner DJ, Hall EJ. Computed tomography – an increasing source of radiation exposure. N Engl J Med 2007;357:2277–84.
[2] Pearce MS, Salotti JA, Little MP, et al. Radiation exposure from CT scans in childhood and subsequent risk of leukaemia and brain tumours: a retrospective cohort study. Lancet 2012;380:499–505.
[3] Marin D, Nelson RC, Samei E, et al. Hypervascular liver tumors: low tube voltage, high tube current multidetector CT during late hepatic arterial phase for detection - initial clinical experience. Radiology 2009;251:771–9.
[4] Nakayama Y, Awai K, Funama Y, et al. Abdominal CT with low tube voltage: preliminary observations about radiation dose, contrast enhancement, image quality, and noise. Radiology 2005;237:945–51.
[5] Nakaura T, Awai K, Oda S, et al. Low-kilovoltage, high-tube-current MDCT of liver in thin adults: pilot study evaluating radiation dose, image quality, and display settings. AJR Am J Roentgenol 2011;196:1332–8.
[6] Yanaga Y, Awai K, Nakaura T, et al. Hepatocellular carcinoma in patients weighing 70 kg or less: initial trial of compact-bolus dynamic CT with low-dose contrast material at 80 kVp. AJR Am J Roentgenol 2011;196:1324–31.
[7] Lee CH, Kim KA, Lee J, et al. Using low tube voltage (80kVp) quadruple phase liver CT for the detection of hepatocellular carcinoma: two-year experience and comparison with Gd-EOB-DTPA enhanced liver MRI. Eur J Radiol 2012;81:e605–11.
[8] Ichikawa T, Motosugi U, Morisaka H, et al. Volumetric low-tube-voltage CT imaging for evaluating hypervascular hepatocellular carcinoma; effects on radiation exposure, image quality, and diagnostic performance. Jpn J Radiol 2013;31:521–9.
[9] Marin D, Nelson RC, Schindera ST, et al. Low-tube-voltage, high-tube-current multidetector abdominal CT: improved image quality and decreased radiation dose with adaptive statistical iterative reconstruction algorithm - initial clinical experience. Radiology 2010;254:145–53.
[10] Hur S, Lee JM, Kim SJ, et al. 80-kVp CT using iterative reconstruction in image space algorithm for the detection of hypervascular hepatocellular carcinoma: phantom and initial clinical experience. Korean J Radiol 2012;13:152–64.
[11] Nakaura T, Nakamura S, Maruyama N, et al. Low contrast agent and radiation dose protocol for hepatic dynamic CT of thin adults at 256-detector row CT: effect of low tube voltage and hybrid iterative reconstruction algorithm on image quality. Radiology 2012;264: 445–54.
[12] Namimoto T, Oda S, Utsunomiya D, et al. Improvement of image quality at low-radiation dose and low-contrast material dose abdominal CT in patients with cirrhosis: intraindividual comparison of low tube voltage with iterative reconstruction algorithm and standard tube voltage. J Comput Assist Tomogr 2012;36:495–501.
[13] Marin D, Choudhury KR, Gupta RT, et al. Clinical impact of an adaptive statistical iterative reconstruction algorithm for detection of hypervascular liver tumours using a low tube voltage, high tube current MDCT technique. Eur Radiol 2013;23:3325–35.
[14] Takahashi H, Okada M, Hyodo T, et al. Can low-dose CT with iterative reconstruction reduce both the radiation dose and the amount of iodine contrast medium in a dynamic CT study of the liver? Eur J Radiol 2014;83:684–91.
[15] Noda Y, Kanematsu M, Goshima S, et al. Reducing iodine load in hepatic CT for patients with chronic liver disease with a combination of low-tube-voltage and adaptive statistical iterative reconstruction. Eur J Radiol 2015;84:11–8.
[16] Zhang X, Li S, Liu W, et al. Double-low protocol for hepatic dynamic CT scan: effect of low tube voltage and low-dose iodine contrast agent on image quality. Medicine 2016;95:e4004.
[17] Juri H, Tsuboyama T, Kumano S, et al. Detection of bladder cancer: comparison of low-dose scans with AIDR 3D and routine-dose scans with FBP on the excretory phase in CT urography. Br J Radiol 2016;89:20150495.
[18] Wallihan DB, Podberesky DJ, Sullivan J, et al. Diagnostic performance and dose comparison of filtered back projection and adaptive iterative dose reduction three-dimensional CT enterography in children and young adults. Radiology 2015;276:233–42.

[19] Onishi H, Kockelkoren R, Kim T, et al. Low-dose pelvic computed tomography using adaptive iterative dose reduction 3-dimensional algorithm: a phantom study. J Comput Assist Tomogr 2015;39:629–34.
[20] Nitta N, Ikeda M, Sonoda A, et al. Images acquired using 320-MDCT with adaptive iterative dose reduction with wide-volume acquisition: visual evaluation of image quality by 10 radiologists using an abdominal phantom. AJR Am J Roentgenol 2014;202:2–12.
[21] Gervaise A, Osemont B, Louis M, et al. Standard dose versus low-dose abdominal and pelvic CT: comparison between filtered back projection versus adaptive iterative dose reduction 3D. Diagn Interv Imaging 2014;95:47–53.
[22] Matsuki M, Murakami T, Juri H, et al. Impact of adaptive iterative dose reduction (AIDR) 3D on low-dose abdominal CT: comparison with routine-dose CT using filtered back projection. Acta Radiol 2013;54:869–75.
[23] Juri H, Matsuki M, Itou Y, et al. Initial experience with adaptive iterative dose reduction 3D to reduce radiation dose in computed tomographic urography. J Comput Assist Tomogr 2013;37:52–7.
[24] Juri H, Matsuki M, Inada Y, et al. Low-dose computed tomographic urography using adaptive iterative dose reduction 3-dimensional: comparison with routine-dose computed tomography with filtered back projection. J Comput Assist Tomogr 2013;37:426–31.
[25] Chen CM, Lin YY, Hsu MY, et al. Performance of adaptive iterative dose reduction 3D integrated with automatic tube current modulation in radiation dose and image noise reduction compared with filtered-back projection for 80-kVp abdominal CT: Anthropomorphic phantom and patient study. Eur J Radiol 2016;85:1666–72.
[26] Chakraborty DP, Berbaum KS. Observer studies involving detection and localization: modeling, analysis, and validation. Med Phys 2004;31:2313–30.
[27] Chakraborty DP. Analysis of location specific observer performance data: validated extensions of the jackknife free-response (JAFROC) method. Acad Radiol 2006;13:1187–93.
[28] Chakraborty DP. Validation and statistical power comparison of methods for analyzing free-response observer performance studies. Acad Radiol 2008;15:1554–66.
[29] Christner JA, Braun NN, Jacobsen MC, et al. Size-specific dose estimates for adult patients at CT of the torso. Radiology 2012;265: 841–7.
[30] American Association of Physicists in Medicine. Size-Specific Dose Estimate (SSDE) in Pediatric and Adult Body CT Examinations (Task Group 204). AAPM, College Park, MD, 2011.
[31] Zachrisson S, Vikgren J, Svalkvist A, et al. Effect of clinical experience of chest tomosynthesis on detection of pulmonary nodules. Acta Radiol 2009;50:884–91.
[32] Nakamoto A, Kim T, Hori M, et al. Clinical evaluation of image quality and radiation dose reduction in upper abdominal computed tomography using model-based iterative reconstruction; comparison with filtered back projection and adaptive statistical iterative reconstruction. Eur J Radiol 2015;84:1715–23.
[33] Singh S, Kalra MK, Hsieh J, et al. Abdominal CT: comparison of adaptive statistical iterative and filtered back projection reconstruction techniques. Radiology 2010;257:373–83.
[34] Schindera ST, Odedra D, Raza SA, et al. Iterative reconstruction algorithm for CT: can radiation dose be decreased while low-contrast detectability is preserved? Radiology 2013;269:511–8.
[35] Jensen K, Martinsen AC, Tingberg A, et al. Comparing five different iterative reconstruction algorithms for computed tomography in an ROC study. Eur Radiol 2014;24:2989–3002.
[36] Schindera ST, Odedra D, Mercer D, et al. Hybrid iterative reconstruction technique for abdominal CT protocols in obese patients: assessment of image quality, radiation dose, and low-contrast detectability in a phantom. AJR Am J Roentgenol 2014;202:W146–52.
[37] McCollough CH, Yu L, Kofler JM, et al. Degradation of CT low-contrast spatial resolution due to the use of iterative reconstruction and reduced dose levels. Radiology 2015;276:499–506.
[38] Nakamoto A, Tanaka Y, Juri H, et al. Diagnostic performance of reduced-dose CT with a hybrid iterative reconstruction algorithm for the detection of hypervascular liver lesions: a phantom study. Eur Radiol 2017;27:2995–3003.